bioRxiv preprint doi: https://doi.org/10.1101/2021.07.02.450857; this version posted July 3, 2021. The copyright holder for this preprint (which was not certified by peer review) is the author/funder. All rights reserved. No reuse allowed without permission.

Title:

Dasabuvir inhibits human norovirus infection in human intestinal enteroids

Authors:

Tsuyoshi Hayashi [1]*, Kosuke Murakami [1], Junki Hirano [1], Yoshiki Fujii [1], Yoko Yamaoka [1], Hirofumi Ohashi [1, 2], Koichi Watashi [1, 2, 3], Mary K. Estes [4], Masamichi Muramatsu [1]*

Affiliation:

1. Department of Virology II, National Institute of Infectious Diseases, Tokyo, Japan
2. Department of Applied Biological Sciences, Tokyo University of Science, Chiba, Japan
3. Research Center for Drug and Vaccine Development, National Institute of Infectious Diseases, Tokyo, Japan
4. Departments of Molecular Virology and Microbiology and of Medicine, Baylor College of Medicine, Houston, Texas, USA

* Correspondence to: Tsuyoshi Hayashi (hayashit@nih.go.jp), Masamichi Muramatsu (muramatsu@nih.go.jp)

Keywords: norovirus; acute gastroenteritis; intestinal enteroids; compound screen; antiviral drug; dasabuvir

bioRxiv preprint doi: https://doi.org/10.1101/2021.07.02.450857; this version posted July 3, 2021. The copyright holder for this preprint (which was not certified by peer review) is the author/funder. All rights reserved. No reuse allowed without permission.

Abstract

Human noroviruses (HuNoVs) are acute viral gastroenteritis pathogens that affect all age groups, yet no approved vaccines and drugs to treat HuNoV infection are available. In this study, with a human intestinal enteroid (HIE) culture system where HuNoVs are able to replicate reproducibly, we screened an antiviral compound library to identify compound(s) showing anti-HuNoV activity. Dasabuvir, which has been developed as an anti-hepatitis C virus agent, was found to inhibit HuNoV infection in HIEs at micromolar concentrations. Dasabuvir also inhibited severe acute respiratory syndrome coronavirus 2 (SARS-CoV-2) and human A rotavirus (RVA) infection in HIEs. To our knowledge, this is the first study to screen an antiviral compound library for HuNoV using HIEs and we successfully identified dasabuvir as a novel anti-HuNoV inhibitor that warrants further investigation.

bioRxiv preprint doi: https://doi.org/10.1101/2021.07.02.450857; this version posted July 3, 2021. The copyright holder for this preprint (which was not certified by peer review) is the author/funder. All rights reserved. No reuse allowed without permission.

Main text:

Human noroviruses (HuNoVs) cause acute gastroenteritis and foodborne diseases among all age groups worldwide. HuNoVs often cause an economic burden to societies due to health care costs and loss of productivity, and therefore pose a public health concern. Noroviruses are non-enveloped viruses possessing a positive sense, single stranded RNA genome whose length is approximately 7.5kb long. They are genetically classified in 10 genogroups (GI-GX) and further divided into 48 genotypes based on their capsid and polymerase gene sequences (Chhabra et al., 2019). Among those, GII.4 genotype is the most frequently distributed and causes outbreak in humans globally (Cannon et al., 2021; Mallory et al., 2019).

Since a robust culture system to allow HuNoV replication was not established for almost 50 years, there is no established treatment options such as vaccines or antiviral regimens available. Recently, several HuNoV successive cultivation models employing a human B cell line (Jones et al., 2014), tissue stem cell-derived human intestinal enteroids (HIEs) (Ettayebi et al., 2016), human induced pluripotent stem cell-derived intestinal organoids (Sato et al., 2019), and zebrafish larvae (Van Dycke et al., 2019) have been developed. The stem cell-derived HIE system is currently used by researchers worldwide to study HuNoV biology and inactivation strategies (Alvarado et al., 2018; Chan et al., 2021; Costantini et al., 2018; Ettayebi et al., 2021; Hosmillo et al., 2020; Lin et al., 2020; Murakami et al., 2020), although, to our knowledge, compound screens for identifying HuNoV antiviral agents have not been reported.

Drug repurposing is a time-saving, affordable strategy to discover new therapeutic uses for approved or developing drugs to treat other disease(s) apart from their original use (Low et al., 2020). This strategy is being widely utilized to establish

bioRxiv preprint doi: https://doi.org/10.1101/2021.07.02.450857; this version posted July 3, 2021. The copyright holder for this preprint (which was not certified by peer review) is the author/funder. All rights reserved. No reuse allowed without permission.

effective therapeutics for treatment of coronavirus disease 2019 (COVID-19). Indeed, numerous antiviral drugs including remdesivir, ivermectin, or nelfinavir has been identified as promising candidates for SARS-CoV-2 (Low et al., 2020; Watashi, 2021). Here, with the HIE culture system, we screened an antiviral compound library composing 326 bioactive substances, including those targeting influenza virus, human immunodeficiency virus (HIV), or Hepatitis C virus (HCV) to reassess their effect on HuNoV infection.

Three dimensional (3D) HIEs were dissociated, and plated on collagen-coated 96 well plates to prepare two-dimensional (2D) monolayers (**Fig. 1A**). The cells were then differentiated by culturing them in differentiation medium, which does not include Wnt3A and R-spondin to support HIE's stemness. The differentiated HIE monolayers were inoculated with GII.4 HuNoV in the presence of each compound dissolved in DMSO for 1 hr at 37^{o}C. DMSO was added to the wells without compound (DMSO control). For this screening step, one well was used to analyze each compound (n = 1). The cells were washed, and cultured in differentiation medium containing the compound for 24 hrs. The infected cells and supernatant were then harvested, and viral replication was evaluated by RT-qPCR analysis to determine the HuNoV RNA genome equivalents (GEs) (**Fig. 1B**). Cytotoxicity for each compound was also determined by LDH assay. First, to evaluate the reproducibility of our HIE system with respect to HuNoV growth throughout the screening, we plotted the level of viral GEs at 1 or 24 hr post-infection (hpi) from 7 independent experiments that were used for the compound screen. The fold changes of viral GEs between 1 and 24 hpi in each experiment ranged from 65 to 230 (mean ± s.d.; 104.3 ± 58.3). A positive control, 2'-C-Methylcytidine (2-CMC) completely blocked viral infection without any cytotoxicity in all experiments, consistent with a previous report (**Fig.**

bioRxiv preprint doi: https://doi.org/10.1101/2021.07.02.450857; this version posted July 3, 2021. The copyright holder for this preprint (which was not certified by peer review) is the author/funder. All rights reserved. No reuse allowed without permission.

1C and D) (Hosmillo et al., 2020). These results demonstrate that our HIE cultivation system reproducibly supports HuNoV replication, and is suitable for evaluating the effect of the compounds against HuNoV.

We next determined the relative percentages of HuNoV GE and cytotoxicity at 24 hpi by normalizing the data of compound-treated cells to DMSO-treated cells. The screening results were plotted as (%) HuNoV GE *vs* (%) Cytotoxicity (**Fig. 1E**). We selected 3 compounds, Dasabuvir (DSB), G243-1637, and 3370-3410, which reduced HuNoV GEs by 95% without cytotoxicity for further validation (**Fig. 1E and Table S1**). For validation purpose, we repeated the experiment with technical 3 replicates and confirmed the reproducible inhibitory effect of DSB and G243-1637 against HuNoV infection (**Fig. S1**). We selected DSB which showed strongest inhibitory effect for further studies. DSB has been developed as one of direct-acting anti-HCV drugs which targets HCV NS5B RNA-dependent RNA polymerase (RdRp) (Trivella et al., 2015). So far, there have been no report regarding any antiviral effects on HuNoV.

Next, we performed additional experiments, with DSB at varying concentrations ranging from 3.125 μM to 50 μM to calculate EC_{50} and CC_{50} values. DSB treatment alone showed no cytotoxicity, except for the highest concentration (50 μM), which showed a 17% reduction of cellular ATPs (cell viability) or 10% increase of LDH release (cytotoxicity), as compared to the DMSO control (**Fig. S2**). Again, DSB did not induce cytotoxicity, except at the highest dose (50 μM) in J2 monolayers infected with GII.4 HuNoV, whereas it showed a dose-dependent inhibition of viral replication with an EC_{50} value of 11.71 μM (**Fig. 2A**). To ascertain the authenticity of DSB's inhibitory effect, we repeated the experiment with the identical compound from different resources and found that the results were comparable (**Fig. S3**). Dose-dependent reduction of viral replication

bioRxiv preprint doi: https://doi.org/10.1101/2021.07.02.450857; this version posted July 3, 2021. The copyright holder for this preprint (which was not certified by peer review) is the author/funder. All rights reserved. No reuse allowed without permission.

by DSB was also observed in J2 HIE monolayers infected with a different HuNoV strain GII.3 (**Fig. 2B)**. We further assessed DSB's inhibitory effect using J3 HIEs established from an independent donor following the infection of GII.3 or GII.4 HuNoV and observed the same trends (**Fig. 2C and D)**. Taken together, DSB exerted an inhibitory effect on two HuNoV genotypes and HIEs established from distinct individuals, strongly suggesting that the effect is neither genotype- nor HIE (donor)-dependent.

Next, we tested the effect of DSB on the infection of human A rotavirus (RVA) and SARS-CoV-2, both of which has been previously reported to be able to infect and replicate HIEs (Lamers et al., 2020; Saxena et al., 2016; Zou et al., 2019). Two concentrations of DSB were used in these studies; non-effective (6.25 μM) and effective concentration (20 μM) against HuNoV, respectively. As shown in **Fig. 3A and B**, DSB showed an antiviral effect (2.75-fold decrease) on RVA infection at a concentration of 20 μM, while it almost completely inhibited (26.9-fold decrease) SARS-CoV-2 infection in J2 HIE monolayers. We also confirmed DSB's inhibition with no cytotoxicity using VeroE6/TMPRSS2 cells which are highly susceptible to SARS-CoV-2 infection (**Figs. 3C, D, and S4**) (Matsuyama et al., 2020).

The mechanism of action for the virus inhibitions by DSB remains to be elucidated. DSB is a non-nucleotide inhibitor of HCV NS5B RdRp that likely binds to palm domain of NS5B and thereby prevents elongation of the nascent viral genome (Kati et al., 2015). Therefore, it might also target the RdRp of other viruses such as HuNoV and SARS-CoV-2, possibly because of the presence of conserved sequences being targeted by DSB. Indeed, there is a report showing that DSB partially inhibits RdRp activity of Middle East respiratory syndrome coronavirus (MERS-CoV) (Min et al., 2020). Targeting viral protease might be another scenario for the inhibition; a very recent virtual

bioRxiv preprint doi: https://doi.org/10.1101/2021.07.02.450857; this version posted July 3, 2021. The copyright holder for this preprint (which was not certified by peer review) is the author/funder. All rights reserved. No reuse allowed without permission.

screening study predicted that dasabuvir has a potential to inhibit 3-chymotrypsin-like protease ($3CL^{PRO}$) of SARS-CoV-2 (Jade et al., 2021).

With a HCV subgenomic replicon system, DSB inhibits HCV of genotype 1 with EC_{50} values of < 10 nM (Kati et al., 2015). In contrast, DSB inhibits HuNoV infection with EC_{50}s ranging between 7.55 and 12.41 μM (**Fig. 2**), which is comparable to its effectiveness to inhibit RdRp activity of MERS-CoV-2 (Min et al., 2020) or infection of vector-borne flaviviruses (Stefanik et al., 2020). This implies that higher concentration is required to exert an antiviral effect on non-HCV viruses, possibly due to lower binding efficiency of DSB to non-HCV RdRp(s) or unknown mechanism of inhibitory action.

In summary, through the screening of an antiviral compound library, we identified DSB as a novel HuNoV inhibitor that warrants further clinical investigation. To our knowledge, this was a first time to identify '*bona fide*' anti-HuNoV agents using the HIE culture system. Our study also shed light on the usefulness of the HIE platform for investigating of anti-HuNoV agents and/or host factors regulating HuNoV infection, which will contribute to better understanding of HuNoV lifecycle and development of vaccine and antiviral regimens.

Acknowledgements

This study was supported by grants from by the Japan Society for the Promotion of Science KAKENHI Grant JP20K07520 (to T.H.); the Japan Agency for Medical Research and Development (AMED) Grants JP21fk0108149 (to K.M. and T.H.), JP21fk0108102 (to M.M. and K.M.), JP21fk0108121 (to K.M.), JP21wm0225009 (to M.M.), JP21fk0108121 (to Y.F.), and NIH Grant PO1 AI057788 (to M.K.E.). We thank Drs.

bioRxiv preprint doi: https://doi.org/10.1101/2021.07.02.450857; this version posted July 3, 2021. The copyright holder for this preprint (which was not certified by peer review) is the author/funder. All rights reserved. No reuse allowed without permission.

Hiroyuki Shimizu, Shutoku Matsuyama and Noriyo Nagata (National Institute of Infectious Diseases) for technical assistance.

Figure legends:

Figure 1. Screening for antiviral compounds that inhibit human norovirus infection in human intestinal enteroids. (A-B) Schematic illustrations of compound screening. Three dimensional HIEs (J2) were trypsinized to single cells, and plated in 96-well plate to culture them as 2D monolayers. Differentiated HIE monolayers were then inoculated with GII.4 HuNoV-containing stool filtrates in the presence of the compounds (10 μM, n=1). After 1 hr incubation at 37°C, the cells were washed, and cultured in differentiation medium containing the compounds (10 μM) in 100 μL volume until 24 hrs post infection (hpi). Viral RNA extracted from the cells and 75 μL of supernatant at 1 or 24 hpi was subjected to RT-qPCR to measure viral genome equivalents (GEs). The rest of the supernatant was subjected to LDH assay to measure cytotoxicity. (C) HuNoV replication in J2 monolayers throughout the screening. We performed 7 experiments to screen all 326 compounds. DMSO and 2'-C-Methylcytidine (2-CMC, 389 μM) were used as controls in every test. Viral GEs in DMSO and 2-CMC treated samples at 24 hpi were normalized to DMSO control at 1 hpi. ** $p < 0.01$ *versus* DMSO control at 24 hpi, one-way ANOVA followed by Dunnett's multiple-comparison test. (D) Cytotoxicity of 2-CMC in J2 monolayers at 24 hpi. Results were normalized to DMSO control. (E) Scatter plot of the % HuNoV GEs *vs* % cytotoxicity for all tested compounds. Results were normalized to DMSO control. Dasabuvir (DSB), red; G243-1637, blue; 3370-3410, green spots.

bioRxiv preprint doi: https://doi.org/10.1101/2021.07.02.450857; this version posted July 3, 2021. The copyright holder for this preprint (which was not certified by peer review) is the author/funder. All rights reserved. No reuse allowed without permission.

Figure 2. Effect of dasabuvir on HuNoV infection in HIE monolayers. J2 (A-B) or J3 (C-D) HIE monolayers were inoculated with GII.4 (A and C) or GII.3 (B and D) HuNoV-containing stool filtrate in the presence of DSB at the indicated concentrations, and were cultured until 20 hpi. The percentages of HuNoV GEs (red lines) and cytotoxicity (blue lines) were determined as in Fig. 1, and were normalized to the DMSO control. Values represent the mean ± s.d. (n ≥ 6). EC_{50}; 50% effective concentration, CC_{50}; 50% cytotoxic concentration.

Figure 3. Dasabuvir inhibits SARS-CoV-2 infection in J2 HIE monolayers and VeroE6/TMPRSS2 cells. (A-B) J2 HIE monolayers were inoculated with RVA (A) and SARS-CoV-2 (B) in the presence of the indicated compounds, and were cultured until 20 hpi. 2-CMC (389 μM) or remdesivir (RDV, 10 μM) were used as positive controls. The percentage of viral GEs were determined by RT-qPCR, and were normalized to the DMSO control at 20 hpi. Values represent the mean ± s.d. (n ≥ 5). (C-D) VeroE6/TMPRSS2 cells were left-uninfected or infected with SARS-CoV-2 for 20 hrs in the presence of the indicated compounds. The cells were then stained with anti-SARS-CoV-2 Spike RBD monoclonal antibody and DAPI followed by imaging analysis. (C) Representative fluorescence images showing SARS-CoV-2 S protein (green) and cell nucleus (blue). Scale bar, 200 μm. (D) The percentages of infected cells were normalized to those of DMSO-treated cells infected with SARS-CoV-2 at 20 hpi. Values represent the mean ± s.d. (n ≥ 8). ** $p < 0.01$ *versus* DMSO control at 20 hpi, one-way ANOVA followed by Dunnett's multiple-comparison test. n.s., not significant ($p > 0.05$).

bioRxiv preprint doi: https://doi.org/10.1101/2021.07.02.450857; this version posted July 3, 2021. The copyright holder for this preprint (which was not certified by peer review) is the author/funder. All rights reserved. No reuse allowed without permission.

Figure S1. Validation of the selected 3 compounds in J2 HIE monolayers. J2 HIE monolayers were inoculated with GII.4 HuNoV-containing stool filtrate in the presence of the indicated compounds (10 μM), and were cultured until 24 hpi. The percentages of HuNoV GEs (A) and cytotoxicity (B) for each compound were determined, as in Fig. 1. Values represent the mean ± s.d. (n ≥ 3). ** $p < 0.01$, * $p < 0.05$ *versus* DMSO control at 24 hpi, two-tailed Student *t* test. n.s., not significant ($p > 0.05$). (C) Chemical structure of Dasabuvir.

Figure S2. Cell viability and cytotoxicity of dasabuvir in J2 HIE monolayers. J2 HIE monolayers were treated with DSB at the indicated concentrations for 20 hr. Cell viability or cytotoxicity was measured using CellTiter-Glo® Luminescent Cell Viability Assay or Cytotoxicity LDH Assay Kit-WST, respectively. Results were normalized to DMSO control. Values represent the mean ± s.d. (n = 7).

Figure S3. Inhibitory effect of dasabuvir purchased from different resources on HuNoV infection in J2 HIE monolayers. J2 HIE monolayers were inoculated with GII.4 HuNoV-containing stool filtrate in the presence of dasabuvir (DSB) purchased from different resources at the indicated concentrations, and cultured until 20 hpi. The percentages of HuNoV GEs and cytotoxicity were determined and were normalized to the DMSO control. Values represent the mean ± s.d. (n = 4).

Figure S4. Cell viability of dasabuvir in VeroE6/TMPRSS2 cells. VeroE6/TMPRSS2 cells were left-uninfected or infected with SARS-CoV-2 for 20 hrs followed by immunofluorescence analysis, as described in Material and Methods. The cell numbers

bioRxiv preprint doi: https://doi.org/10.1101/2021.07.02.450857; this version posted July 3, 2021. The copyright holder for this preprint (which was not certified by peer review) is the author/funder. All rights reserved. No reuse allowed without permission.

were determined by counting cell nucleus. Results were normalized to DMSO-treated cells infected with SARS-CoV-2. Values represent the mean ± s.d. (n = 8).

Table S1. Compound screening results. The percentages of HuNoV GEs and cytotoxicity in the presence of the indicated compound (10 μM, n=1) were determined and normalized to those of DMSO control.

References

Alvarado, G., Ettayebi, K., Atmar, R.L., Bombardi, R.G., Kose, N., Estes, M.K., Crowe, J.E., Jr., 2018. Human Monoclonal Antibodies That Neutralize Pandemic GII.4 Noroviruses. Gastroenterology 155, 1898-1907.

Cannon, J.L., Bonifacio, J., Bucardo, F., Buesa, J., Bruggink, L., Chan, M.C., Fumian, T.M., Giri, S., Gonzalez, M.D., Hewitt, J., Lin, J.H., Mans, J., Muñoz, C., Pan, C.Y., Pang, X.L., Pietsch, C., Rahman, M., Sakon, N., Selvarangan, R., Browne, H., Barclay, L., Vinjé, J., 2021. Global Trends in Norovirus Genotype Distribution among Children with Acute Gastroenteritis. Emerg Infect Dis 27, 1438-1445.

Chan, J.C.M., Mohammad, K.N., Zhang, L.-Y., Wong, S.H., Chan, M.C.-W., 2021. Targeted Profiling of Immunological Genes during Norovirus Replication in Human Intestinal Enteroids. Viruses 13, 155.

Chhabra, P., de Graaf, M., Parra, G.I., Chan, M.C., Green, K., Martella, V., Wang, Q., White, P.A., Katayama, K., Vennema, H., Koopmans, M.P.G., Vinjé, J., 2019. Updated classification of norovirus genogroups and genotypes. J Gen Virol 100, 1393-1406.

Costantini, V., Morantz, E.K., Browne, H., Ettayebi, K., Zeng, X.L., Atmar, R.L., Estes, M.K., Vinjé, J., 2018. Human Norovirus Replication in Human Intestinal Enteroids as Model to Evaluate Virus Inactivation. Emerg Infect Dis 24, 1453-1464.

Ettayebi, K., Crawford, S.E., Murakami, K., Broughman, J.R., Karandikar, U., Tenge, V.R., Neill, F.H., Blutt, S.E., Zeng, X.L., Qu, L., Kou, B., Opekun, A.R., Burrin, D.,

bioRxiv preprint doi: https://doi.org/10.1101/2021.07.02.450857; this version posted July 3, 2021. The copyright holder for this preprint (which was not certified by peer review) is the author/funder. All rights reserved. No reuse allowed without permission.

255 Graham, D.Y., Ramani, S., Atmar, R.L., Estes, M.K., 2016. Replication of human
256 noroviruses in stem cell-derived human enteroids. Science 353, 1387-1393.
257 Ettayebi, K., Tenge, V.R., Cortes-Penfield, N.W., Crawford, S.E., Neill, F.H., Zeng,
258 X.L., Yu, X., Ayyar, B.V., Burrin, D., Ramani, S., Atmar, R.L., Estes, M.K., 2021. New
259 Insights and Enhanced Human Norovirus Cultivation in Human Intestinal Enteroids.
260 mSphere 6.
261 Hosmillo, M., Chaudhry, Y., Nayak, K., Sorgeloos, F., Koo, B.K., Merenda, A., Lillestol,
262 R., Drumright, L., Zilbauer, M., Goodfellow, I., 2020. Norovirus Replication in Human
263 Intestinal Epithelial Cells Is Restricted by the Interferon-Induced JAK/STAT Signaling
264 Pathway and RNA Polymerase II-Mediated Transcriptional Responses. mBio 11.
265 Jade, D., Ayyamperumal, S., Tallapaneni, V., Joghee Nanjan, C.M., Barge, S., Mohan,
266 S., Nanjan, M.J., 2021. Virtual high throughput screening: Potential inhibitors for SARS-
267 CoV-2 PL(PRO) and 3CL(PRO) proteases. Eur J Pharmacol 901, 174082.
268 Jones, M.K., Watanabe, M., Zhu, S., Graves, C.L., Keyes, L.R., Grau, K.R., Gonzalez-
269 Hernandez, M.B., Iovine, N.M., Wobus, C.E., Vinjé, J., Tibbetts, S.A., Wallet, S.M.,
270 Karst, S.M., 2014. Enteric bacteria promote human and mouse norovirus infection of B
271 cells. Science 346, 755-759.
272 Kati, W., Koev, G., Irvin, M., Beyer, J., Liu, Y., Krishnan, P., Reisch, T., Mondal, R.,
273 Wagner, R., Molla, A., Maring, C., Collins, C., 2015. In vitro activity and resistance
274 profile of dasabuvir, a nonnucleoside hepatitis C virus polymerase inhibitor. Antimicrob
275 Agents Chemother 59, 1505-1511.
276 Lamers, M.M., Beumer, J., van der Vaart, J., Knoops, K., Puschhof, J., Breugem, T.I.,
277 Ravelli, R.B.G., Paul van Schayck, J., Mykytyn, A.Z., Duimel, H.Q., van Donselaar, E.,
278 Riesebosch, S., Kuijpers, H.J.H., Schipper, D., van de Wetering, W.J., de Graaf, M.,
279 Koopmans, M., Cuppen, E., Peters, P.J., Haagmans, B.L., Clevers, H., 2020. SARS-
280 CoV-2 productively infects human gut enterocytes. Science 369, 50-54.
281 Lin, S.C., Qu, L., Ettayebi, K., Crawford, S.E., Blutt, S.E., Robertson, M.J., Zeng, X.L.,
282 Tenge, V.R., Ayyar, B.V., Karandikar, U.C., Yu, X., Coarfa, C., Atmar, R.L., Ramani, S.,
283 Estes, M.K., 2020. Human norovirus exhibits strain-specific sensitivity to host interferon
284 pathways in human intestinal enteroids. Proc Natl Acad Sci U S A 117, 23782-23793.
285 Low, Z.Y., Farouk, I.A., Lal, S.K., 2020. Drug Repositioning: New Approaches and
286 Future Prospects for Life-Debilitating Diseases and the COVID-19 Pandemic Outbreak.
287 Viruses 12.
288 Mallory, M.L., Lindesmith, L.C., Graham, R.L., Baric, R.S., 2019. GII.4 Human
289 Norovirus: Surveying the Antigenic Landscape. Viruses 11.

bioRxiv preprint doi: https://doi.org/10.1101/2021.07.02.450857; this version posted July 3, 2021. The copyright holder for this preprint (which was not certified by peer review) is the author/funder. All rights reserved. No reuse allowed without permission.

290 Matsuyama, S., Nao, N., Shirato, K., Kawase, M., Saito, S., Takayama, I., Nagata, N.,
291 Sekizuka, T., Katoh, H., Kato, F., Sakata, M., Tahara, M., Kutsuna, S., Ohmagari, N.,
292 Kuroda, M., Suzuki, T., Kageyama, T., Takeda, M., 2020. Enhanced isolation of SARS-
293 CoV-2 by TMPRSS2-expressing cells. Proc Natl Acad Sci U S A 117, 7001-7003.
294 Min, J.S., Kim, G.W., Kwon, S., Jin, Y.H., 2020. A Cell-Based Reporter Assay for
295 Screening Inhibitors of MERS Coronavirus RNA-Dependent RNA Polymerase Activity.
296 J Clin Med 9.
297 Murakami, K., Tenge, V.R., Karandikar, U.C., Lin, S.C., Ramani, S., Ettayebi, K.,
298 Crawford, S.E., Zeng, X.L., Neill, F.H., Ayyar, B.V., Katayama, K., Graham, D.Y.,
299 Bieberich, E., Atmar, R.L., Estes, M.K., 2020. Bile acids and ceramide overcome the
300 entry restriction for GII.3 human norovirus replication in human intestinal enteroids.
301 Proc Natl Acad Sci U S A 117, 1700-1710.
302 Sato, S., Hisaie, K., Kurokawa, S., Suzuki, A., Sakon, N., Uchida, Y., Yuki, Y., Kiyono,
303 H., 2019. Human Norovirus Propagation in Human Induced Pluripotent Stem Cell-
304 Derived Intestinal Epithelial Cells. Cell Mol Gastroenterol Hepatol 7, 686-688.e685.
305 Saxena, K., Blutt, S.E., Ettayebi, K., Zeng, X.L., Broughman, J.R., Crawford, S.E.,
306 Karandikar, U.C., Sastri, N.P., Conner, M.E., Opekun, A.R., Graham, D.Y., Qureshi,
307 W., Sherman, V., Foulke-Abel, J., In, J., Kovbasnjuk, O., Zachos, N.C., Donowitz, M.,
308 Estes, M.K., 2016. Human Intestinal Enteroids: a New Model To Study Human
309 Rotavirus Infection, Host Restriction, and Pathophysiology. J Virol 90, 43-56.
310 Stefanik, M., Valdes, J.J., Ezebuo, F.C., Haviernik, J., Uzochukwu, I.C., Fojtikova, M.,
311 Salat, J., Eyer, L., Ruzek, D., 2020. FDA-Approved Drugs Efavirenz, Tipranavir, and
312 Dasabuvir Inhibit Replication of Multiple Flaviviruses in Vero Cells. Microorganisms 8.
313 Trivella, J.P., Gutierrez, J., Martin, P., 2015. Dasabuvir: a new direct antiviral agent for
314 the treatment of hepatitis C. Expert Opinion on Pharmacotherapy 16, 617-624.
315 Van Dycke, J., Ny, A., Conceição-Neto, N., Maes, J., Hosmillo, M., Cuvry, A.,
316 Goodfellow, I., Nogueira, T.C., Verbeken, E., Matthijnssens, J., de Witte, P., Neyts, J.,
317 Rocha-Pereira, J., 2019. A robust human norovirus replication model in zebrafish
318 larvae. PLoS Pathog 15, e1008009.
319 Watashi, K., 2021. Identifying and repurposing antiviral drugs against severe acute
320 respiratory syndrome coronavirus 2 with in silico and in vitro approaches. Biochem
321 Biophys Res Commun 538, 137-144.
322 Zou, W.Y., Blutt, S.E., Crawford, S.E., Ettayebi, K., Zeng, X.L., Saxena, K., Ramani, S.,
323 Karandikar, U.C., Zachos, N.C., Estes, M.K., 2019. Human Intestinal Enteroids: New
324 Models to Study Gastrointestinal Virus Infections. Methods Mol Biol 1576, 229-247.

325

Figure 1

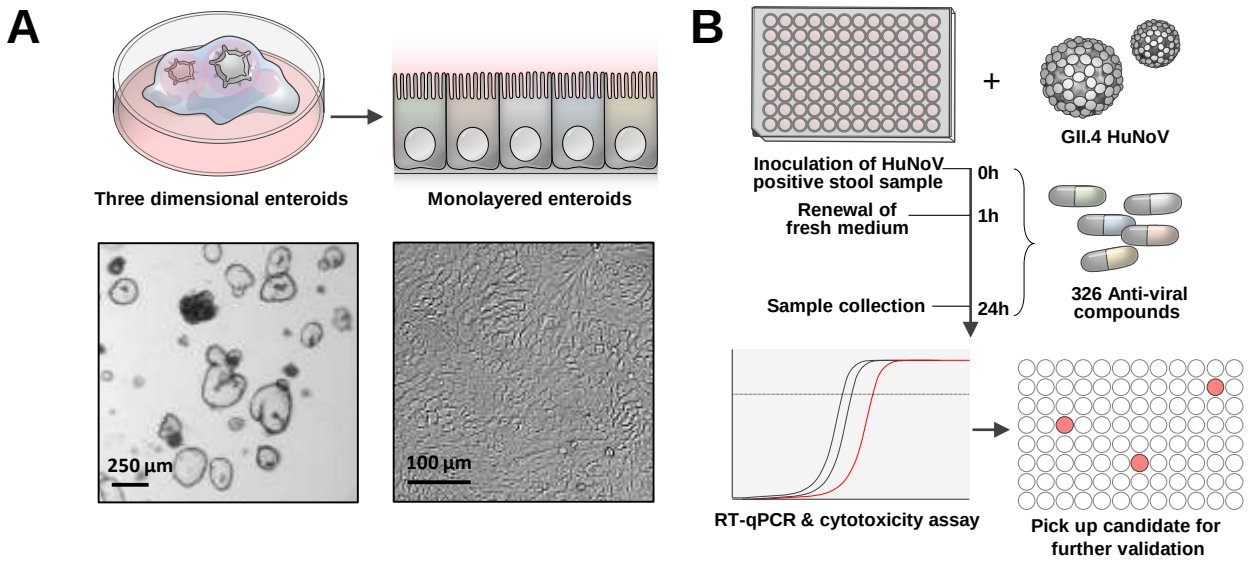
A
Three dimensional enteroids
Monolayered enteroids
250 μm
100 μm
B
+
GII.4 HuNoV
Inoculation of HuNoV positive stool sample
0h
Renewal of fresh medium
1h
Sample collection
24h
326 Anti-viral compounds
RT-qPCR & cytotoxicity assay
Pick up candidate for further validation

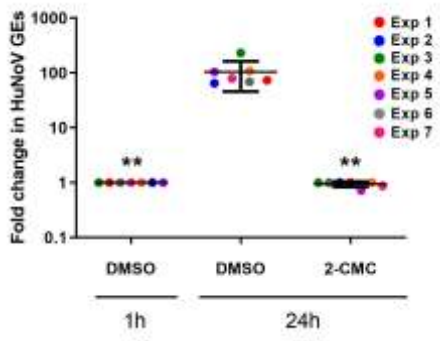
C
Fold change in HuNoV GEs
1000
100
10
1
0.1
**
**
Exp 1
Exp 2
Exp 3
Exp 4
Exp 5
Exp 6
Exp 7
DMSO
DMSO
2-CMC
1h
24h

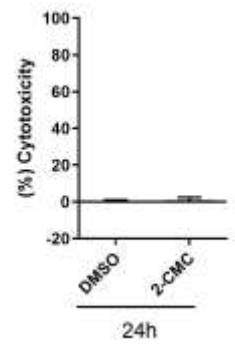
D
(%) Cytotoxicity
100
80
60
40
20
0
-20
DMSO
2-CMC
24h

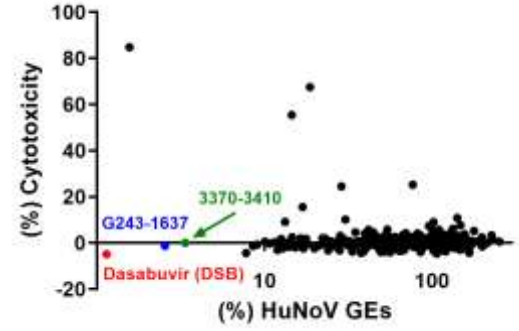
E
(%) Cytotoxicity
100
80
60
40
20
0
-20
3370-3410
G243-1637
Dasabuvir (DSB)
10
100
(%) HuNoV GEs

Figure 2

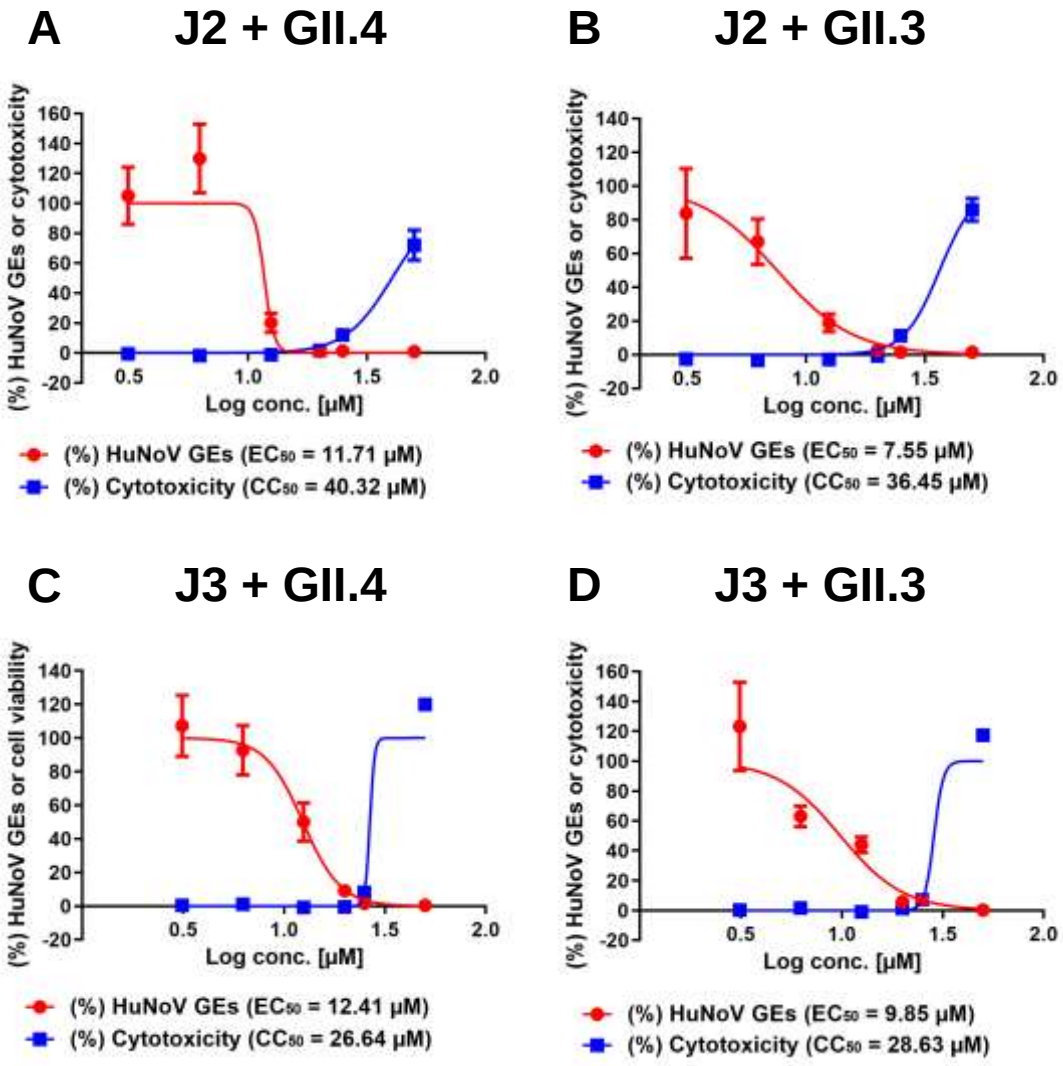
A
J2 + GII.4
(%) HuNoV GEs or cytotoxicity
Log conc. [μM]
(%) HuNoV GEs (EC50 = 11.71 μM)
(%) Cytotoxicity (CC50 = 40.32 μM)
B
J2 + GII.3
(%) HuNoV GEs or cytotoxicity
Log conc. [μM]
(%) HuNoV GEs (EC50 = 7.55 μM)
(%) Cytotoxicity (CC50 = 36.45 μM)
C
J3 + GII.4
(%) HuNoV GEs or cell viability
Log conc. [μM]
(%) HuNoV GEs (EC50 = 12.41 μM)
(%) Cytotoxicity (CC50 = 26.64 μM)
D
J3 + GII.3
(%) HuNoV GEs or cytotoxicity
Log conc. [μM]
(%) HuNoV GEs (EC50 = 9.85 μM)
(%) Cytotoxicity (CC50 = 28.63 μM)

Figure 3

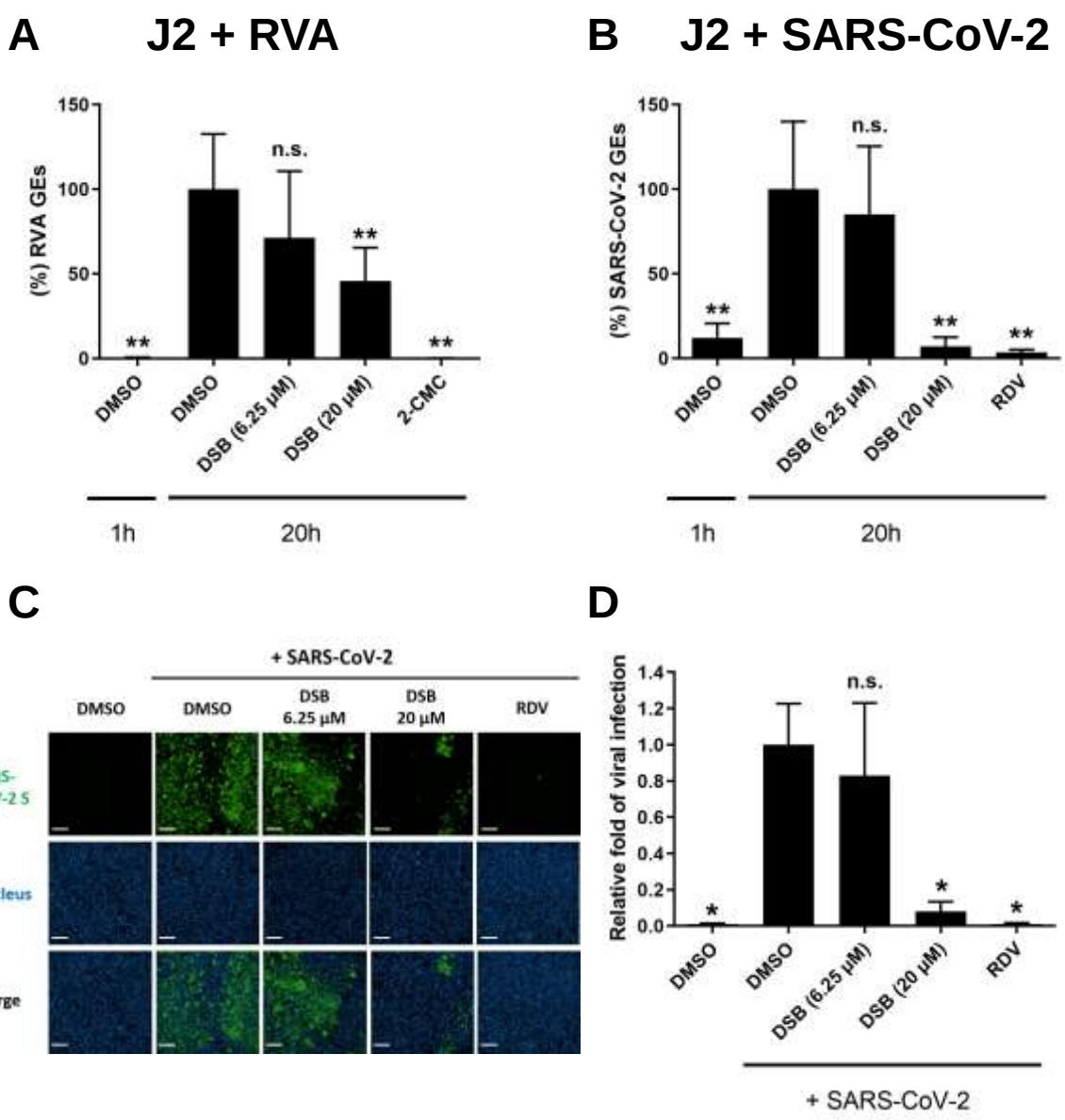
A
J2 + RVA
(%) RVA GEs
150
100
50
0
n.s.
**
**
**
DMSO
DMSO
DSB (6.25 µM)
DSB (20 µM)
2-CMC
1h
20h
B
J2 + SARS-CoV-2
(%) SARS-CoV-2 GEs
150
100
50
0
n.s.
**
**
**
DMSO
DMSO
DSB (6.25 µM)
DSB (20 µM)
RDV
1h
20h
C
+ SARS-CoV-2
DMSO
DMSO
DSB 6.25 µM
DSB 20 µM
RDV
SARS-CoV-2 S
Nucleus
Merge
D
Relative fold of viral infection
1.4
1.2
1.0
0.8
0.6
0.4
0.2
0.0
n.s.
*
*
*
DMSO
DMSO
DSB (6.25 µM)
DSB (20 µM)
RDV
+ SARS-CoV-2

Figure S1

A

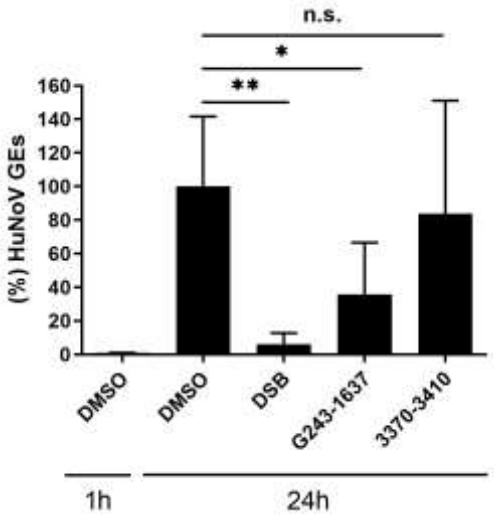

B

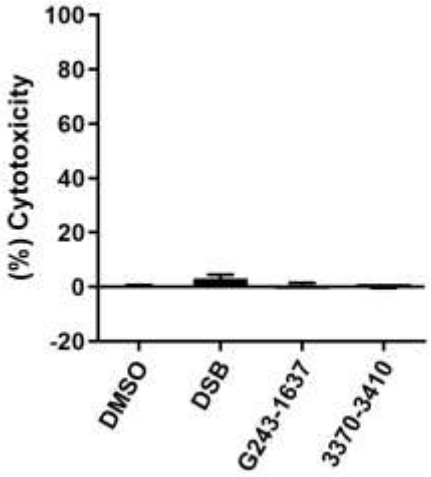

C

Dasabuvir (DSB)

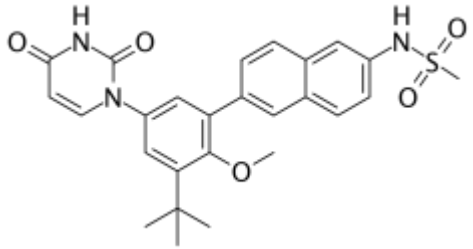

Figure S2

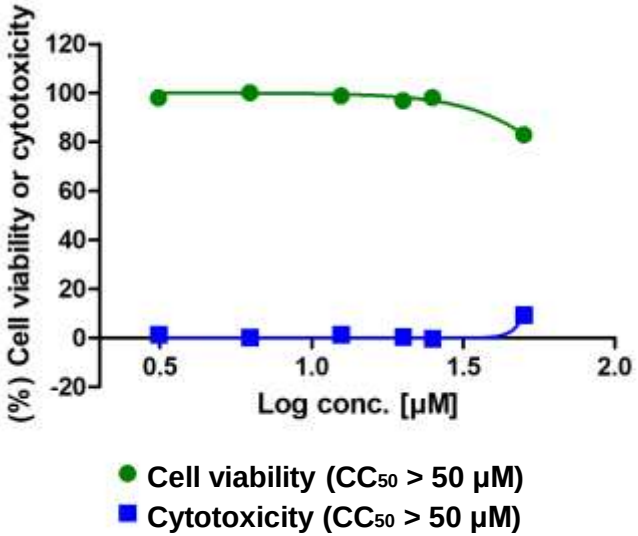
(%) Cell viability or cytotoxicity
120
100
80
60
40
20
0
-20
0.5
1.0
1.5
2.0
Log conc. [μM]
Cell viability (CC50 > 50 μM)
Cytotoxicity (CC50 > 50 μM)

Figure S3

A DSB (Selleck, S5402)

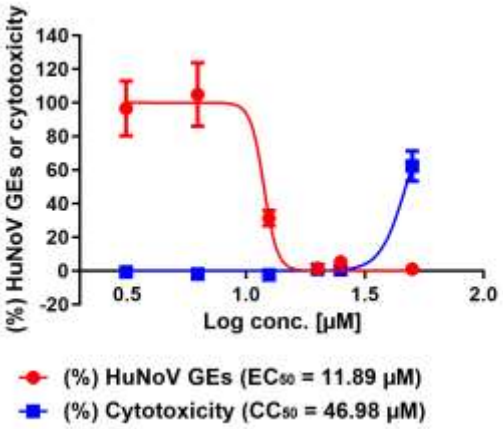

B DSB (Cayman Chemical, 18482)

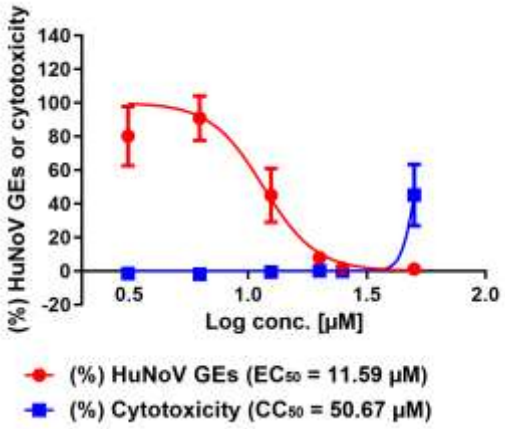

Figure S4

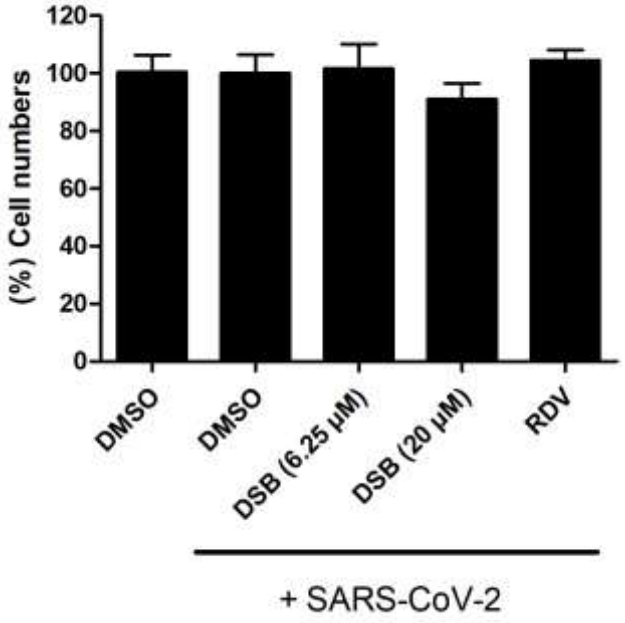
120
100
80
60
40
20
0
(%) Cell numbers
DMSO
DMSO
DSB (6.25 μM)
DSB (20 μM)
RDV
+ SARS-CoV-2

Table S1

Compound	(%) HuNoV GEs	(%) Cytotoxicity
Dasabuvir	1.14	-4.83
AG-1478	1.56	84.88
G243-1637	2.54	-1.23
3370-3410	3.36	0.00
Oltipraz	7.76	-4.37
Dolutegravir	8.52	-1.39
D128-0609	9.02	-0.67
Cefotaxime sodium	10.06	0.51
Y070-3535	10.72	-0.22
K978-0113	11.46	0.34
4778-0092	11.93	0.09
Oleanonic Acid	11.94	-3.05
Enoxacin	12.49	0.62
Y030-6944	12.51	-1.89
Y031-1132	12.56	1.79
Floxuridine	12.64	0.65
C547-0919	12.83	-2.30
8018-5978	12.89	-0.12
Triciribine	13.24	9.12
6540-0274	13.95	0.34
Voriconazole	14.05	-1.63
Crystal Violet	14.53	55.49
E155-0203	14.58	2.50
5436-1131	15.22	-1.95
Amprenavir	15.87	-0.21
Betulinic acid	16.39	2.09
Arbidol hydrochloride	16.88	15.58
D389-0267	17.01	-2.35
Merimepodib	17.03	0.74
R092-0019	17.68	1.84
E565-0914	18.05	-0.45
Geldanamycin	18.63	67.53
Cobicistat	19.83	-2.34
Ethidium bromide	21.15	-1.16
Penciclovir	22.14	2.02
Valacyclovir hydrochloride	22.45	0.09
Diammonium Glycyrrhizinate	22.61	0.23
Sofosbuvir	22.63	0.74
Wiskostatin	22.91	2.02
Entecavir hydrate	23.60	-1.04
E582-0206	23.81	0.09
1,2,3,4,6-O-Pentagalloylglucose	23.98	-3.29
8020-0349	24.10	-1.70
Dapivirine	24.80	0.74
Y030-9081	25.30	-0.21
5829-8232	26.13	-1.42
Y031-2258	27.09	0.90
Famciclovir	27.31	0.72
1630-0616	27.33	-1.90
Fluorouracil	27.42	-0.47

2377-0618	27.91	-0.77
Azlocillin sodium	28.00	-1.98
C276-0156	28.06	-3.25
Vagistat	28.28	3.16
Etravirine	28.81	24.52
Oxethazaine	29.35	1.91
0233-0085	29.46	2.03
D090-0045	30.38	10.15
Cytarabine	31.34	-0.77
7567-0240	31.82	-1.15
Turofexorate Isopropyl	31.93	0.86
Guanosine	32.26	0.15
Doravirine	32.68	-1.39
E461-0189	33.20	-0.26
7472-0163	33.47	-3.79
Clevudine	33.75	-0.09
Adenosine 5'-monophosphate monohydrate	34.38	0.18
Brivudine	34.83	4.68
0509-0350	34.99	0.43
C528-0431	35.15	-1.34
C260-2491	35.51	0.35
4456-2665	35.77	0.63
Y030-9422	36.07	-0.35
HZ-1157	36.74	0.70
D715-1039	37.50	-0.09
8014-8659	37.68	-4.37
Y030-9216	39.06	-0.96
Bay 41-4109 racemate	39.26	-3.52
Ilaprazole sodium	39.34	1.57
Nelfinavir Mesylate	39.67	4.06
Tizoxanide	39.97	2.28
Dehydroandrographolide Succinate Potasium Salt	40.48	-2.10
K786-6982	40.91	0.34
C256-1592	40.91	-1.57
Rimantadine hydrochloride	40.94	2.41
Tinidazole	41.02	-0.09
C517-4132	41.72	-0.69
Y031-0424	41.78	5.76
Cefixime	41.90	2.28
D178-0176	42.09	0.56
G243-0866	42.35	0.52
Phthalylsulfathiazole	44.00	2.05
Nitazoxanide	44.54	4.63
Inositol	44.92	2.88
Paritaprevir	44.98	-0.33
8010-1605	45.00	0.09
0611-0108	45.12	-0.92
D715-0622	45.64	0.70
D044-0078	45.84	1.04
Oxytetracycline	46.16	3.05
Y031-2476	46.31	1.68
Dermofongin	46.93	-0.74

6321-0204	48.24	-0.43
Trovirdine	48.30	-2.69
Selonsertib	48.46	-2.58
8015-6196	49.03	0.90
C279-0863	49.22	0.44
Raltegravir	49.31	1.45
8017-8518	49.34	-3.92
E848-0049	49.53	-1.26
Sulfadoxine	49.98	2.36
C281-0111	50.00	-1.15
Pirodavir	50.55	-3.64
6872-1469	50.87	0.43
Vidarabine	51.42	-2.58
Artemisinin	51.67	1.63
Osalmid	52.08	3.16
5941-1200	52.40	-3.79
Forsythin	52.42	1.24
C527-0619	52.56	-2.35
Orotic acid	52.58	0.45
Maraviroc	52.60	-1.98
Y031-4822	52.62	0.56
Y030-3795	52.65	1.56
Ritonavir	52.68	1.11
Didanosine	52.78	-0.07
Telaprevir	53.18	0.86
C677-0056	53.38	3.79
E565-0873	53.67	0.09
Cabotegravir	54.14	5.83
YYA-021	54.17	-1.15
Aciclovir	54.44	0.59
C241-1871	54.62	-2.41
C848-0358	54.70	0.52
Tenofovir alafenamide	55.19	-0.20
Iohexol	55.34	1.11
C085-2292	55.42	1.13
Emtricitabine	55.47	2.80
C857-1956	55.72	0.72
Vitamin E Acetate	55.75	1.21
Oxymatrine	56.15	2.33
E793-3695	56.38	-4.02
Tenofovir	56.45	0.98
Nevirapine	56.63	0.72
C328-0243	56.69	0.78
Zidovudine	57.57	0.59
KIN1148	58.10	0.52
4223-6713	58.85	2.22
Nandrolone decanoate	58.93	0.98
Dichlorisone Acetate	59.14	-1.58
Velpatasvir	59.83	1.45
Limonin	59.90	0.73
Y041-2092	60.06	1.30
Rifampicin	60.21	2.64
G856-4392	60.30	1.04

C470-0438	60.97	1.13
C547-0142	61.21	0.09
Amenamevir	61.67	0.09
E243-0077	61.92	-2.53
Lonafarnib	62.33	1.84
K786-5923	62.64	1.00
Fluensulfone	63.19	-2.22
5782-5821	63.42	1.56
Dexchlorpheniramine Maleate	63.62	-3.40
5991-0006	64.26	-1.68
Pritelivir	64.49	-1.63
Ribavirin	64.55	-0.09
Abacavir	64.88	0.27
6321-0334	65.13	-3.45
2512-0260	65.73	0.70
Chloroxylenol	65.87	1.68
Atazanavir	66.38	0.72
C700-1353	66.68	-2.24
Adefovir dipivoxil	67.07	3.59
Dendrid	67.26	-0.36
Xanthohumol	67.33	2.40
G243-1720	68.21	-3.02
8004-9093	68.82	-1.39
C270-0058	69.28	-1.15
Betulin	69.81	4.24
Y041-2077	70.07	2.78
Telbivudine	70.21	-0.33
C677-0152	70.48	-0.69
Beta-Cyclodextrin	70.60	-0.91
MGL3196	70.80	-0.56
K780-0942	70.93	0.78
Andrographolide	70.94	-1.18
5991-0071	71.37	0.45
Zalcitabine	71.45	2.88
4072-2560	72.37	-0.52
G847-0104	72.73	-0.45
D051-0007	75.02	0.46
Y031-0201	75.43	-0.26
4270-0405	75.84	-1.22
8010-6143	75.89	-0.17
Resiquimod	76.69	2.61
Miconazole	76.75	25.21
Trifluridine	77.12	0.46
Y030-4666	77.23	1.13
8015-2049	78.12	-1.72
Rolipram	78.65	-0.46
K286-0899	78.94	2.12
Favipiravir	80.97	-1.51
E521-1399	81.36	-0.34
Oleanolic Acid	82.04	4.14
C700-1366	83.21	2.09
Patchouli alcohol	83.87	1.24
C466-0437	84.93	2.53

4896-3719	85.51	-3.91
Salicylanilide	85.53	1.82
Clemizole	85.68	3.11
Y041-1917	85.81	-1.61
Fostemsavir	87.35	-2.34
Lomibuvir	87.62	-1.75
Foscarnet sodium	88.54	1.07
1349-0002	90.28	0.96
Dicurone	90.75	1.49
C519-2093	90.86	0.26
Darunavir	91.79	0.74
K786-8151	93.07	-1.12
Y030-6369	95.25	1.82
Econazole	95.76	7.35
C528-0945	96.16	-0.90
Ebselen	96.70	2.77
Baicalin	97.70	1.68
7752-0085	98.30	0.78
1630-1692	99.02	-0.35
E535-6327	99.93	1.01
Ampicillin Trihydrate	99.95	1.14
Ethambutol dihydrochloride	100.33	0.23
C795-0720	100.75	0.72
Naringin	100.79	5.67
Des(benzylpyridyl) Atazanavi	101.09	2.40
Lopinavir	101.84	9.07
8015-2125	102.00	3.68
8014-9100	102.04	-3.33
Mecarbinate	102.13	0.93
Glycyrrhizin	102.52	4.28
C466-0389	102.90	0.57
D043-0313	103.02	1.26
C226-3999	103.27	-0.46
Catalpol	104.47	3.07
G008-1418	104.79	0.70
R052-0761	104.95	1.95
8017-8512	106.48	-4.70
Erythromycin ethylsuccinate	106.62	0.23
6321-0504	107.80	-2.76
Tetracycline	108.05	0.09
Spectinomycin dihydrochloride	109.17	-1.44
Y020-7585	109.80	1.00
K832-4216	109.98	5.71
6872-1644	111.18	-3.33
D715-0631	111.30	-1.49
K783-0395	112.04	-0.92
6641-0204	112.44	-2.91
8011-7669	112.53	-0.12
Spermine	115.70	2.77
Cefepime Dihydrochloride Monohydrate	116.48	3.73
Ganciclovir	117.43	3.59
Rilpivirine	117.49	0.20
Lamivudine	118.04	0.86

Cefdinir	118.35	2.33
K788-8290	118.67	1.22
Moroxydine hydrochloride	119.22	-1.11
E570-0242	119.50	0.87
E207-1342	120.58	-3.68
Y041-3934	120.81	1.49
8011-6210	121.01	0.56
6064-0094	121.40	-2.02
Stavudine	123.60	2.15
C226-3957	123.88	-0.34
Vitamin E	125.47	-0.33
7706-1060	125.74	-1.05
Y070-3375	126.02	1.00
C527-0550	130.07	4.71
C328-0429	130.84	2.26
E734-2662	131.61	0.80
6526-0824	131.97	2.41
Ledipasvir acetone	133.29	6.17
G855-2047	133.69	-2.02
Efavirenz	134.78	1.69
C301-6874	139.45	1.56
8013-2327	139.52	-2.35
8015-3915	140.84	0.26
Verdinexor	141.53	10.81
C618-0871	142.69	-1.49
PSI6206	143.70	3.20
6214-0789	143.78	-0.22
C697-0280	144.66	-2.24
G402-0939	147.17	1.01
C328-0222	147.26	1.90
5282-1184	147.35	-2.91
Y031-2490	147.45	1.56
8011-7237	147.64	7.61
Darunavir Ethanolate	147.86	-0.07
6228-0891	147.93	-0.87
E717-0652	148.85	0.96
C677-0057	155.51	-0.35
6466-0862	155.85	-0.22
C719-0236	156.11	-2.18
8009-6815	156.54	3.81
C075-0149	157.54	0.45
G402-0849	158.24	1.12
Clotrimazole	158.66	0.51
K940-1348	160.80	-0.11
Bicyclol	161.99	0.26
K286-3667	162.45	0.07
Elvitegravir	163.99	0.85
Naringenin	164.68	1.14
C697-0502	166.44	-4.26
6321-0438	166.79	-3.79
6872-0590	169.40	-0.34
C430-0518	170.30	-1.01
Isoliquiritigenin	172.34	0.86

Daclatasvir dihydrochloride	178.20	5.28
8014-1990	179.78	0.61
Valganciclovir hydrochloride	188.71	0.33
E975-1597	190.33	0.56
Emricasan	198.22	1.13
(-)-Epigallocatechin Gallate	198.37	2.41
C050-0346	198.78	-1.57
E461-0584	204.16	-0.90
Revaprazan hydrochloride	214.12	0.20
G404-0515	226.81	3.36
Amantadine hydrochloride	231.71	1.24
Aloe-emodin	253.04	0.59